Current Research in Food Science 10 (2025) 100973

Contents lists available at ScienceDirect

Current Research in Food Science

journal homepage: www.sciencedirect.com/journal/current-research-in-food-science

Exploring the contribution of phosphatidylcholine and triglyceride on the formation of beef aroma-active compounds with thermal oxidation system

Yujie Shi [a,b,1], Jing Li [a,b,1], Longzhu Zhou [b], Junmin Zhang [b], Xiaohui Feng [b], Weihai Xing [b], Chaohua Tang [b,*], Yueyu Bai [a,**]

[a] School of Agricultural Sciences, Zhengzhou University, Zhengzhou, 450001, China
[b] State Key Laboratory of Animal Nutrition and Feeding, Institute of Animal Sciences of Chinese Academy of Agricultural Sciences, Beijing, 100193, China

ARTICLE INFO

Handling Editor: Professor Aiqian Ye

Keywords:
Phosphatidylcholine
Defatted beef matrix
Lipid oxidation
Flavoromics
Thermal oxidation model reconstruction

ABSTRACT

Thermal oxidation of phospholipids and triglycerides is a major source of beef aroma compounds. In this study, phosphatidylcholine (PC) and triglyceride (TG) were isolated and purified from beef and added to defatted beef and raw beef. The composition of aroma compounds generated by thermal oxidation in three model systems were compared by flavoromics. The main aroma compounds produced by the thermal oxidation of PC were decanal, (E)-2-nonenal, (E)-2-undecenal, and (E,E)-2,4-decadienal, while the main aroma compounds produced by the thermal oxidation of TG were nonanal, (E)-2-undecenal, and decanal. Nonanal remains the main aroma compound produced by PC and TG in defatted beef. Octanal and nonanal were the major aroma compounds generated by thermal oxidation of raw beef samples spiked with PC and TG. Raw beef with added PC and TG had higher levels of sulfides and heterocycles after thermal oxidation compared to defatted beef with added lipids. The comparison of the aroma profiles in three thermo-oxidative models indicated that PC contributed more than TG to the key odor-active compounds in cooked beef. Additionally, the thermo-oxidative degradation of PC facilitated the formation of Maillard reaction products. However, the beef matrix may inhibit the formation of decanal and (E,E)-2,4-decadienal.

1. Introduction

Beef is the predominant high-quality meat product in human daily life. Aroma is a crucial determinant of beef's edible quality and an essential reference indicator for consumers assessing preference level (Miller et al., 2023; O'quinn et al., 2024). Lipid thermal oxidation degradation may contribute significantly to the overall aroma of cooked meat. The most abundant aroma compounds in cooked meat from lipid oxidation are short-chain saturated aldehydes (C_6-C_{10}), 1-octen-3-ol (or 1-octen-3-one), and sulfur containing compounds or Nitrogen-containing compounds, which exert the strongest influence on meat aroma (Sohail et al., 2022). Important odor-active compounds in beef included (E,E)-2,4-Decadienal, nonanal, 2,3-octanedione, acetoin, 2-pentylfuran, 1-octen-3-ol, and pentanal, compounds often associated with lipid oxidation(Cui et al., 2023; Zhou et al., 2024). Additionally, the interaction between lipid degradation and the Maillard reaction, known as the lipid-Maillard interaction, plays an important role in the formation of meat aroma (Elmore and Mottram, 2006). The 2,4-hexadienal generated from the thermo-oxidative degradation of fat/oxidized fat participates in glutathione-glucose reaction, leading to the formation of 2-ethylthiophene (Zhao et al., 2019). Lipid thermal oxidation is the primary pathway for the formation of key aroma compounds in cooked beef.

Beef intramuscular fat consists mainly of triglyceride (TG) and phospholipids. Studies have shown that phospholipids play an important role in the generation of characteristic aromas of beef (Mottram and Edwards, 1983). The content and types of lipid oxidation derivatives are closely related to the polarity of the lipids. The addition of phosphatidylcholine (PC) promotes the formation of pyrazine, the characteristic aroma compound of hot air-dried shrimp, thereby inhibiting the formation of trimethylamine, a key component of the fishy smell (Zheng et al., 2025). Thermal oxidation modeling of individual lipids in vitro

* Corresponding author.
** Corresponding author.
E-mail addresses: tangchaohua@cass.cn (C. Tang), baiyueyu666@sina.com (Y. Bai).
[1] These authors contributed equally to this work and should be considered co-first.

https://doi.org/10.1016/j.crfs.2025.100973
Received 13 September 2024; Received in revised form 2 December 2024; Accepted 7 January 2025
Available online 17 January 2025

can be used to analyze the effects of thermo-oxidative degradation of phospholipids on aroma formation (Chen et al., 2023). The composition of muscle tissue is complex, and the meat matrix may affect odorant interactions, which in turn alters the aroma of cooked meat (Wang et al., 2024). Zhang et al. constructed an interaction oxidation model of myofibrillar proteins, polar and non-polar lipid in different ratios found that increasing the specific gravity of polar lipids favored the formation of the characteristic aroma of large yellow croaker (Zhang et al., 2024). This suggests that matrix modeling could be employed to investigate the mechanisms of aroma formation.

The thermo-oxidative degradation of lipids within the meat matrix is a complex process. Previous studies have analyzed the effect of lipid oxidation on aroma compounds using lipid standards or explored the correlation between volatiles and lipids through bioinformatics analysis. However, thermal oxidation modeling of the reconstruction of the matrix has not been employed to examine the ability of lipids to produce aroma compounds in cooked beef. PC and TG were extracted and isolated from raw beef. Additionally, defatted beef matrices were prepared. Three experimental groups were designed for this study: a single lipid in vitro thermal oxidation model, a lipid-defatted beef reconstitution thermal oxidation model, and a lipid-raw beef thermal oxidation model. The aims of this study were: 1) to compare three thermo-oxidative models to investigate the effects of PC and TG thermo-oxidative degradation on the key odor-active compounds in cooked beef and their interactions with the Maillard reaction, 2) to elucidate the effect of beef matrices on the formation of aroma compounds during lipid thermo-oxidative degradation using a defatted beef matrix reconstruction thermal oxidation model and a raw beef thermal oxidation model. This study may provide a theoretical basis for investigating the mechanism by which thermo-oxidative degradation of lipid molecules contributes to the formation of characteristic beef aroma compounds.

2. Methods and materials

2.1. Sample preparation

This study followed the Guidelines for the use of Experimental Animals established by the Ministry of Science and Technology (Beijing, China). All experimental protocols were approved by the Science Research Department of the Institute of Animal Sciences, Chinese Academy of Agricultural Sciences (Beijing, China) (No. IAS2024-104). The beef was purchased from Pingdingshan Ruibao Red Beef Industry Co., Ltd. (Henan, China). Jiaxian red cattle were fed for 30 months with a fattening period of 15 ± 3 months. The feed formula was shown in Table S1. After the feeding period, all cattle passed quarantine inspection and were transported to commercial slaughterhouses. They were fasted for 24 h prior to slaughter and then humanely slaughtered by professional personnel. The process included electric stunning, bleeding, evisceration, and splitting of the carcass along the midline. After slaughter, the cattle carcasses were drained of acid at 0–4 °C for 72 h. The sirloins were vacuum packed and stored at −20 °C and transported to the laboratory for testing.

2.2. Total lipids extraction

The extraction of total lipid from beef was referenced according to the method described by Matyash (Matyash et al., 2008). 0.3 mL of methanol was added to 65 mg sample and homogenized (60 Hz, 60 s). Afterwards 1.0 mL of methyl tertiary butyl ether was added, the mixture was shaken. Further, 250 μL of ultrapure water was added to the tube, the mixture was shaken. The samples were centrifuged (8000g, 4 °C, 10min). The upper phase was transferred to a new tube and brought to dryness under a gentle nitrogen stream.

2.3. Phospholipids separation and purification

Briefly, the extracted crude total lipids were separated into different classes on silicic acid columns (25 cm × 2.5 cm i. d., 35 g of Si 60 silica gel, particle size 200–300 μm, Yuanye). The PC and TG fractions were obtained (Saito, 2007). The fractions were then concentrated under reduced pressure and stored at −80 °C until thin layer chromatography and ultra-performance liquid chromatography quadrupole time-of-flight mass spectrometry. Photo of thin layer plate was taken by a smartphone (Xiaomi, China).

2.4. Preparation of defatted beef and raw beef matrix reaction models

Firstly, defatted beef matrices were prepared by removing total fat from beef twice with dichloromethane: methanol (2:1, v/v). Then methyl tertiary butyl ether: methanol (3:1, v/v) was add to remove total lipids three times. Finally, defatted beef matrices were freeze-dried for 24h.

The samples were divided into three groups.

Group 1: Thermal oxidation modelling of single lipids in vitro.
(1) PC sample (PC): 0.01g of PC.
(2) TG sample (TG): 0.01g of TG.

Group 2: Reconstructed thermal oxidation modelling of defatted beef with the addition of PC or TG (DF-Lipids).
(1) Defatted beef sample (DF): 1g defatted beef.
(2) Defatted beef with PC sample (DF-PC): 0.01g of PC, 1g defatted beef.
(3) Defatted beef with TG sample (DF-TG): 0.01g of TG, 1g defatted beef.

Group 3: Thermal oxidation modelling of raw beef with the addition of PC or TG (RB-Lipids).
(1) Raw beef sample (RB): 1g raw beef.
(2) Raw beef with PC sample (RB-PC): 0.01g of PC, 1g raw beef.
(3) Raw beef with TG sample (RB-TG): 0.01g of TG, 1g raw beef.

All samples were placed in 20 mL glass vials and heated in a boiling water bath (100 °C, 30 min), then in an ice water bath for 5 min. Every sample had three replications in the experiment.

2.5. Gas chromatography-olfactometry mass spectrometry (GC-O-MS) analysis

Samples were mixed with 10 μL 2-methyl-3-heptanone (0.01 μg/μL in Methanol). The vial was tightly capped with a silicon-polytetrafluoroethylene septum, and incubated for 20 min at 55 °C. Volatile compounds were extracted for 40 min at the same time using a SPME fiber tip (50/30 μm, divinylbenzene/carboxen/polydimethylsiloxane) from Sigma Aldrich(USA) and desorbed for 3 min at 250 °C. Volatile compounds were analyzed on a Q-Exactive-GC-Orbitrap-MS (Thermo Fisher Scientific, USA) equipped with a VF-WAXms capillary column (60 m × 0.25 mm × 0.25 μm, Agilent, USA). The carrier gas was high-purity helium at a flow rate of 2.0 mL/min and a split ratio of 1:1. The column temperature was initially set to 40 °C, increased to 230 °C at 4 °C/min, and held for 5 min at 230 °C. Mass spectrometry parameters: full scan mode; electron impact ion source; electron energy 70 eV; mass range: 30–400 m/z; ion source 280 °C; transmission line 250 °C. Sniffing port parameters: sniffing port 90 °C; sniffing transmission line 250 °C.

The GC-O-MS system was consisted of a GC-MS system with an olfactometer detector (Gerstel, Germany). The sample was desorbed through the injection, separated by GC, and then entered the mass spectrometry detector and the olfactory detector port respectively with the split ratio of 1:1. For GC-O analysis, 3 experts aged between 20 and 25 years old were selected, all of whom have extensive experience in GC-O analysis or have received over 6 months of training. 4-Point scale was

utilized to record retention times, odor descriptors, and odor intensity values (Lu et al., 2024).

Volatile compounds were identified by comparison with mass spectra from the NIST 2.0 and Wiley libraries, linear retention indices. Linear retention indices were calculated by a series of n-alkanes (C_7-C_{40}) under the same detection conditions and compared to the literature to confirm the identified compounds. In addition, the sniffed compounds were reconfirmed based on standard odor descriptions. Finally, the identified compounds were verified using the existing standards. Each volatile compound was calculated by comparing the peak area of the compound with that of 2-methyl-3-heptanone according to Qi et al. (2022).

2.6. Odor activity value (OAV) calculation

Based on the semi-quantification of various aroma compounds in Section 2.5, regarding the threshold value of each compound in water, the OAV value of aroma compounds was calculated using the following formula(Cui et al., 2023):

$$OAV_i = C_i / OT_i \quad (1)$$

Where OAV_i is the aroma activity value of compound i, C_i is the mass concentration of compound i in μg/kg, and OT_i is the aroma threshold of compound i in water (μg/kg), which is obtained from Gemert (2011). ODOR THRESHOLDS. Odor threshold values in water (Chapter 2).

2.7. Ultra performance liquid chromatography-quadrupole-time of flight-mass spectrometry analysis (UPLC-Q-TOF-MS)

The UPLC system was coupled to a Q-TOF-MS instruments (AB SCIEX 6600, USA) equipped with an electrospray ionization probe. Two fractions were separated on a Waters HSS T3 column (2.1 mm × 50 mm, Waters, USA). A binary solvent system was used, in which mobile phase A consisted of 10 mM ammonium formate in acetonitrile: distilled water (60:40, v/v), and mobile phase B was 10 mM ammonium formate in isopropanol: acetonitrile (90:10, v/v). The mobile phase gradient was as follows: 0–6 min (100%A-0%B, 0.3 mL/min); 6–30 min (50%A-50%B, 0.3 mL/min); 30–32 min (0%A-100%B, 0.3 mL/min); 32–35 min (100% A-0%B, 0.3 mL/min).

Electrospray ionization (ESI) was used to detect positive and negative ions. The parameters of the ion source were set as follows: MS1 scan m/z range: 100–1200 Da, MS2 scan m/z range: 50–1200 Da; turbo source gun temperature, 500 °C; spray voltage, 5500 V (ESI) and −4500 V (ESI); curtain gas pressure, 35 psi; gas 1 pressure, 50 psi; gas 2 pressure, 50 psi. Lipid molecules were identified by MExplorer Ultimate software (Mestrelab Research, ES). The lipids with a chromatographic area > 10^7 were considered as a confident identification.

2.8. Statistical analysis

The relevant results were denoted as mean ± SD. Statistical analysis was performed using SPSS (SPSS 20.0 for Windows, SPSS Inc.). Principal component analysis was performed using SIMCA 14.1. Venn Plots were

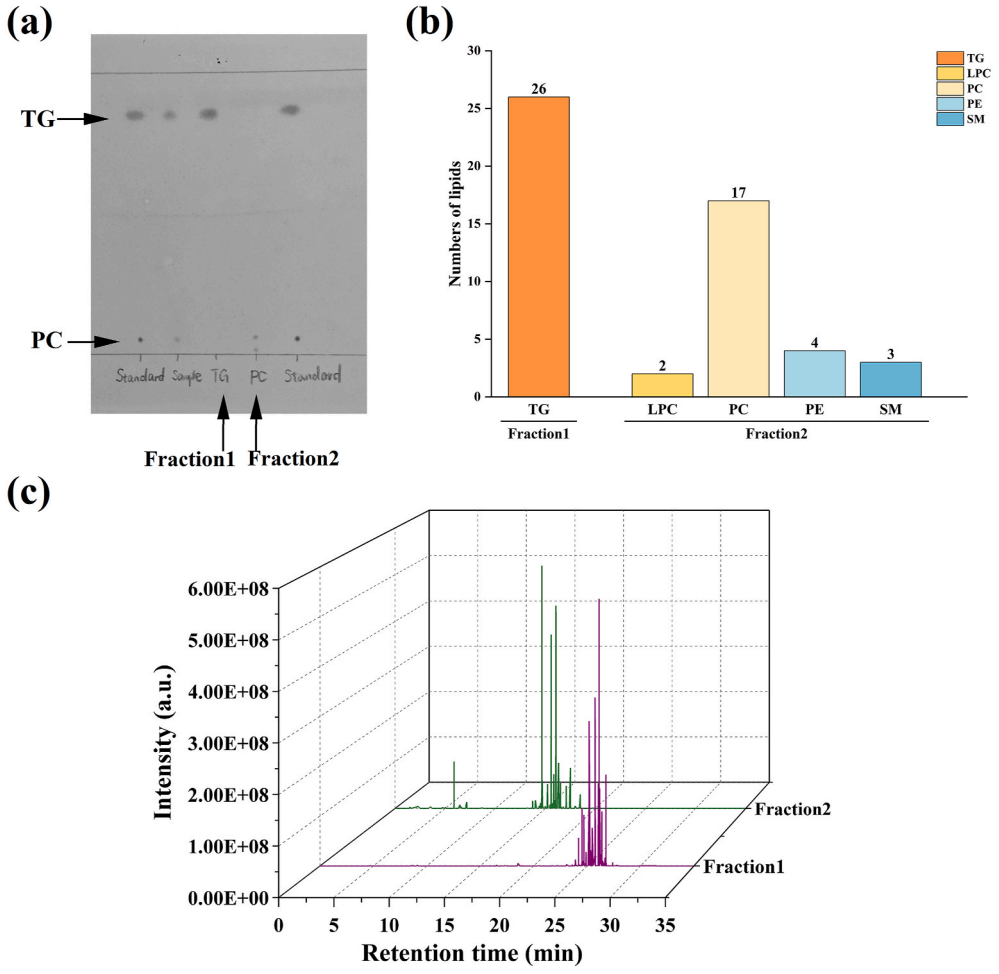

Fig. 1. (a) Graphical representation of a chemically revealed thin layer chromatography plate of PC and TG separated from beef. (b) Numbers of PC and TG molecules in fraction 1 and fraction 2. (c) 3D total ion chromatogram of UPLC–Q–TOF–MS in full scan positive ion mode of PC and TG molecules separated from beef.

drawn using Draw Venn Plot (http://bioinformatics.psb.ugent.be/webtools/Venn). Heatmap analysis was performed using the OmicShare tools (https://www.omicshare.com/tools). Bar charts, chord plot and sunburst chart were drawn by Origin (2024) software.

3. Results

3.1. Identification of PC and TG molecules

PC and TG in beef had been separated as identified by thin layer chromatography (Fig. 1(a)). The total ion chromatograms based on the [M+H] ion peak in the PC sample and the [M + NH_4] ion peak in the TG sample are shown in Fig. 1(c). In the extracted total lipids from beef, 26 TG molecules (fraction 1) and 26 phospholipids molecules (fraction 2) were isolated (Fig. 1(b)). Fraction 1 consisted of 26 molecules of triglycerides, while fraction2 comprised 17 phosphatidylcholine, 2 lysophosphatidylcholine, 4 phosphatidylethanolamine, and 3 sphingomyelin (Table S2). Analysis using UPLC-Q-TOF-MS revealed that PC (P-16:0/18:1), PC (16:0/18:1), and PC (P-16:0/18:2) were the major PC molecules isolated from beef. TG (16:0/18:1/18:1), TG (16:1/18:1/18:1), TG (14:0/18:1/18:1) and TG (16:0/17:1/17:1) were the major TG molecules isolated from beef.

3.2. Comparison of the aroma-active compounds produced by PC and TG oxidation

Venn plot analysis revealed 49 aroma compounds were common to both PC and TG, with (E)-2-nonenal exclusively detected in heated PC, while hexanoic acid, 2-heptanone, citronellyl acetate and α-pinene were exclusively found in heated TG (Fig. 2(a)). Principal component analysis of the aroma compounds generated from heating PC and TG revealed that the cumulative contribution rate of the first two principal components reached 88% (Fig. 2(b)). There were distinct differences observed in the aroma compounds produced from TG and PC. As shown in Table 1, total of 54 aroma compounds were detected in beef PC and TG, of which 21 aldehydes, 9 ketones and 5 lactones (Fig. 2(c)). The total concentration of aldehydes and esters detected from heated TG was notably higher than heated PC, whereas PC exhibited significantly higher levels of ketones compared to TG (Fig. 2(d)).

Nonanal, decanal and (E,E)-2,4-decadienal were identified as the primary aldehydes generated from PC and TG thermal oxidation in beef. Decanal and (E,E)-2,4-decadienal content was significantly higher in heated PC compared to TG, whereas nonanal content was eight times higher in heated TG than in PC. 2-Nonanone and 2-decanone were identified as the principal ketones formed upon lipid heating, with higher levels of 2-nonanone and 2-decanone generated from PC thermal oxidation compared to TG. Lactones were identified as the primary esters formed during thermal oxidation of beef PC and TG, with notably higher levels of γ-nonalactone generated from PC heating. The OAV method was used to evaluate the odor-active compounds identified in the PC and TG thermal oxidation samples. 14 Odor-active compounds with OAV>1 were identified by GC-O technique in heated PC and 11 in heated TG (Table 2). These odor-active compounds could be classified into aliphatic aldehydes and ketones. (E, E)-2,4-decadienal was the odor-active compound with the highest OAV in heated PC (OAV = 4846.07) and 1-octen-3-one was the odor-active compound with the highest OAV in heated TG (OAV = 2371.04).

3.3. Comparison the aroma-active compounds in the model constructed with defatted matrix and lipid class

Principal Component Analysis was conducted on aroma compounds generated from defatted beef samples, revealing that the cumulative contribution rate of the first two principal components was 94.4% (Fig. 3(a)). As shown in Fig. 3(b), aldehydes were the most abundant species produced by the thermal reactions of DF-PC and DF-TG. A total of 61 aroma compounds were identified in DF-PC and DF-TG samples, with aldehydes being the most abundant species (Fig. 3(d)). As shown in Fig. 3(c), lipid addition significantly increased the content of various aroma compounds in heated defatted beef samples, with aldehydes,

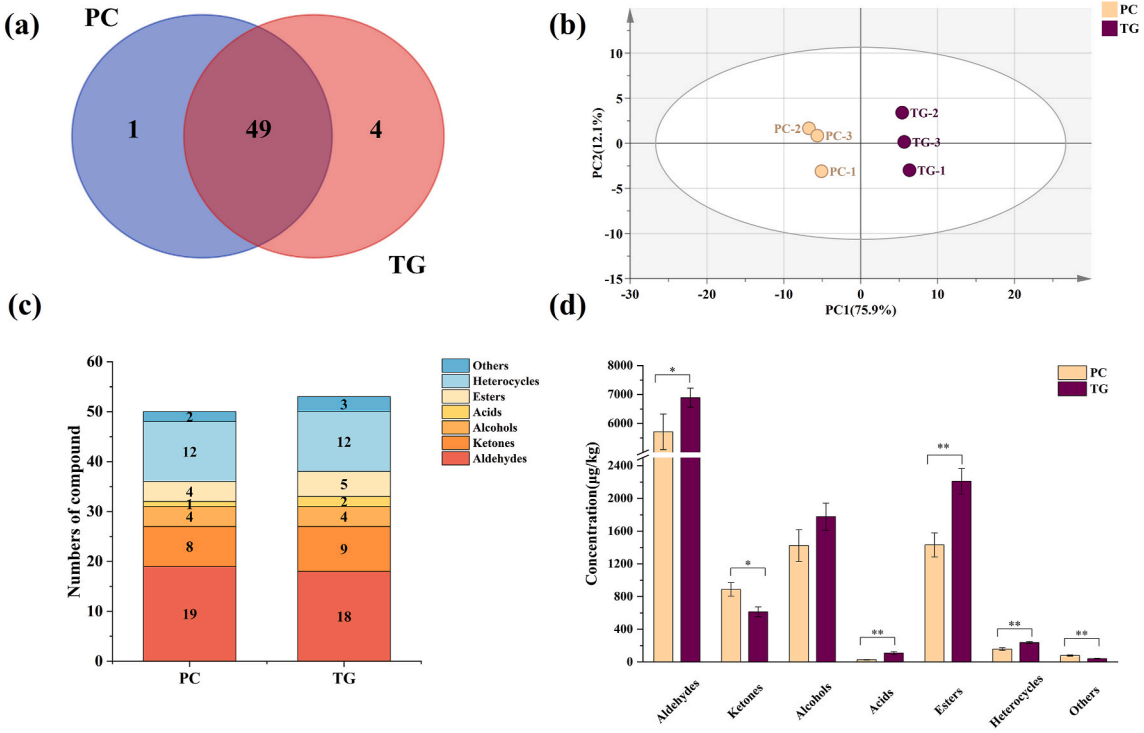

Fig. 2. Analysis of aroma compounds generated by thermal oxidation of PC and TG. (a)Venn plot analysis of aroma compounds. (b) Two-dimensional PCA score plot. (c) The numbers of aroma compounds. (d) The concentration of aroma compounds.

Table 1
Mean values of the aroma compounds identified in heated lipids samples (n = 3).

No.	Component name	LRI[1]		Identification method[4]	Lipids samples (μg/kg)		Lipid sig[6]
		Calculated[2]	Literature[3]		PC[5]	TG[5]	
Aldehydes							
1	Butanal	882	883	MS,RI,S	7.67 ± 1.93	4.39 ± 0.26	*
2	Pentanal	986	979	MS,RI,S	5.88 ± 0.6	1.88 ± 0.2	***
3	Hexanal	1088	1077	MS,RI,S,O	12.78 ± 1.1	2.13 ± 0.4	***
4	Heptanal	1184	1182	MS,RI,S,O	39.61 ± 5.82	20.28 ± 3.15	**
5	(E)-2-Hexenal	1220	1216	MS,RI,S,O	26.51 ± 0.69	16.66 ± 5.34	*
6	Octanal	1287	1298	MS,RI,S,O	62.89 ± 8.11	50.03 ± 31.89	ns
7	(E)-2-Heptenal	1323	1323	MS,RI,S	9.66 ± 1.45	1.45 ± 0.22	**
8	Nonanal	1389	1402	MS,RI,S,O	325.67 ± 43.26	2459.25 ± 152.98	***
9	(E)-2-Octenal	1425	1429	MS,RI,S,O	176.56 ± 16.11	100.96 ± 21.95	**
10	(E,E)-2,4-Heptadienal	1488	1495	MS,RI,S,O	13.21 ± 1.28	7.04 ± 1.49	**
11	Decanal	1491	1508	MS,RI,S,O	1878.55 ± 321.52	861.3 ± 39.76	**
12	Benzaldehyde	1518	1541	MS,RI,S	1085.93 ± 15.91	1921.17 ± 74.35	***
13	(E)-2-Nonenal	1528	1534	MS,RI,S,O	343.95 ± 40.6	nd	**
14	2-Methylbenzaldehyde	1618	1632	MS,RI	40.09 ± 0.86	160.22 ± 26.83	**
15	(E)-2-Decenal	1635	1644	MS,RI,S,O	22.09 ± 3.13	128.81 ± 20.86	**
16	4-Ethylbenzaldehyde	1732	1759	MS,RI,S	41.06 ± 6.2	94.84 ± 5.51	***
17	(E)-2-Undecenal	1741	1752	MS,RI,S,O	642.72 ± 75.87	608.37 ± 50.02	ns
18	(E,E)-2,4-Decadienal	1798	1811	MS,RI,S,O	969.21 ± 192.95	411.2 ± 23.73	**
19	Cinnamaldehyde	2023	2018	MS,RI,S	7.75 ± 1.85	36.77 ± 1.45	***
Ketones							
20	2-Pentanone	984	981	MS,RI	nd	46.05 ± 4.58	***
21	2-Heptanone	1183	1190	MS,RI,S	17.64 ± 3.23	15.47 ± 3.57	ns
22	3-Octanone	1252	1253	MS,RI,S	111.97 ± 14.09	190.8 ± 13.78	**
23	Acetoin	1288	1284	MS,RI,S,O	33.98 ± 5.36	23.23 ± 4.82	ns
24	1-Octen-3-one	1298	1310	MS,RI,S,O	62.07 ± 6.82	37.94 ± 6.6	*
25	6-Methyl-5-hepten-2-one	1333	1338	MS,RI,S	16.88 ± 2.68	18.64 ± 1.87	ns
26	2-Nonanone	1385	1397	MS,RI,S	436.38 ± 37.96	143.26 ± 32.77	**
27	3-Octen-2-one	1402	1411	MS,RI,S	45.66 ± 7.71	39.62 ± 6.82	ns
28	2-Decanone	1486	1494	MS,RI,S,O	162.91 ± 27.2	98.21 ± 22.73	*
Alcohols							
29	Decanol	1740	1760	MS,RI,S	642.71 ± 75.86	608.37 ± 50.02	ns
30	Benzenemethanol	1852	1880	MS,RI,S	334.07 ± 55.76	204.16 ± 27.45	*
31	Benzeneethanol	1936	1926	MS,RI,S	25.12 ± 5.04	58.03 ± 3.47	**
32	Dodecanol	1939	1969	MS,RI,S	422.57 ± 63.44	905.79 ± 89.07	
Acids							
33	Pentanoic acid	1715	1733	MS,RI	27.73 ± 2.21	20.19 ± 1.35	**
34	Hexanoic acid	1819	1846	MS,RI,S	nd	88.21 ± 16.97	**
Esters							
35	Citronellyl acetate	1625	1660	MS,RI,S	nd	497.22 ± 31.71	***
36	γ-Hexalactone	1694	1723	MS,RI,S	207.9 ± 25.51	266.07 ± 76.77	ns
37	γ-Heptanolactone	1792	1817	MS,RI,S	527.99 ± 70.94	545.22 ± 22.26	ns
38	γ-nonalactone	2013	2024	MS,RI,S	676.54 ± 60.66	431.18 ± 41.86	**
39	γ-Undecalactone	2239	2259	MS,RI,S	19.3 ± 4.19	470.09 ± 55.58	***
Heterocycles							
40	2-Methylfuran	874	869	MS,RI	2.14 ± 0.16	12.91 ± 0.73	***
41	2-Butylfuran	1126	1123	MS,RI	0.95 ± 0.07	4.22 ± 0.24	***
42	2-Pentylfuran	1227	1241	MS,RI,S,O	3.4 ± 0.44	4.5 ± 0.4	*
43	Methylpyrazine	1266	1266	MS,RI,S	6.49 ± 1.03	3.81 ± 1.34	ns
44	2-Ethylpyridine	1280	1278	MS,RI	7.45 ± 0.64	0.44 ± 0.12	***
45	2-Hexylfuran	1326	1321	MS,RI	23.45 ± 1.69	24.18 ± 4.87	ns
46	2-Pentythiophene	1455	1448	MS,RI,S	9.3 ± 1.45	8.89 ± 1.63	ns
47	2-Pentylpyridine	1564	1584	MS,RI,S	67.57 ± 7.44	87.14 ± 2.62	*
48	2-Acetylpyridine	1595	1597	MS,RI,S	8.92 ± 0.68	24.18 ± 2.93	**
49	2-Acetylthiazole	1636	1643	MS,RI	1.57 ± 0.36	2.45 ± 0.3	*
50	2-Acetylpyrrole	1946	1973	MS,RI,S	13.48 ± 1.58	40.28 ± 3.71	***
51	Coumarin	2433	2454	MS,RI,S	13.94 ± 2.22	24.79 ± 1.31	**
Others							
52	Benzene	948	957	MS,RI	2.12 ± 0.16	0.44 ± 0.15	***
53	α-Pinene	1031	1015	MS,RI,S	nd	5.93 ± 0.65	***
54	Styrene	1257	1270	MS,RI,S	77.62 ± 7.68	34.7 ± 3.78	**

nd, not detected. PC, phosphatidylcholine; TG, triglyceride.
1 Linear retention index.
2 Calculated data based on a homologous series of n-alkanes (C_7-C_{40}).
3 Data obtained from the online database: http://www.flavornet.org/, https://pubchem.ncbi.nlm.nih.gov/.
4 MS, identified using MS spectra; RI, identified using the linear retention index; S, confirmed by comparison with authentic standards; O, confirmed by olfactory confirmation.
5 Different letters in the same row represent significant differences($p < 0.05$).
6 Difference between means; ns = no significant difference between means; *, ** and *** indicate significant differences at $p < 0.05$, $p < 0.01$ and $p < 0.001$, respectively.

Table 2
Odor activity values (OAVs) of important odor-active compounds in Heated Lipids Samples, Defatted Beef Samples, and Raw Beef Samples (n = 3).

No.	Compounds[1]	Sensory threshold (μg/kg)[2]	Odor descriptors	OAV Value							
				PC	TG	DF	DF-PC	DF-TG	RB	RB-PC	RB-TG
1	Pentanal	12	green, malt, pungent	nd	nd	nd	nd	nd	9.11	35.49	16.25
2	Dimethyl disulfide	1.20	onion, cabbage	nd	nd	3.66	74.01	36.56	70.46	111.34	86.52
3	Hexanal	2.78	green, fresh grass	4.60	<1	1.12	40.93	3.56	126.69	149.90	140.15
4	Heptanal	2.80	fat, citrus	14.15	7.24	26.85	91.37	59.61	110.49	111.90	89.56
5	(E)-2-Hexenal	17.00	green, fatty	1.56	<1	<1	2.20	<1	1.62	3.41	1.27
6	2-Pentylfuran	5.80	green bean, butter	<1	<1	2.30	6.63	6.06	6.86	11.36	8.68
7	Octanal	3.40	green, citrus, lemon	18.50	14.71	7.73	38.44	31.37	317.48	615.65	488.12
8	Acetoin	14.00	butter, cream	2.43	1.66	<1	13.15	6.11	2.58	3.54	2.83
9	1-Octen-3-one	0.02	mushroom	3879.58	2371.04	<1	4956.04	1593.75	5261.25	10376.67	6966.88
10	Dimethyl trisulfide	0.10	sulfury, meaty	nd	nd	20.80	610.17	210.13	1873.13	3984.70	1324.23
11	Nonanal	2.80	citrus, green	116.31	878.30	<1	1048.05	1229.27	357.45	717.33	897.39
12	(E)-2-Octenal	3.00	fat, nut	58.85	33.65	<1	20.08	17.62	12.87	11.28	16.19
13	Methional	0.20	cooked potato	nd	nd	nd	nd	nd	23.00	379.77	336.07
14	2-Decanone	3.00	heavy, sweet	54.30	32.74	1.31	218.68	70.12	1.67	6.32	4.66
15	(E,E)-2,4-Heptadienal	15.40	green, spicy	<1	<1	nd	nd	nd	1.45	6.92	4.88
16	Decanal	3.00	fatty, meaty, burnt	626.18	287.10	2.73	63.05	72.50	9.35	14.71	18.96
17	(E)-2-Nonenal	0.19	cucumber, fat, green	1810.28	<1	<1	801.54	305.63	718.33	1736.05	994.35
18	(E)-2-Decenal	0.30	green, tallow	73.63	429.36	32.33	129.99	164.24	245.74	424.32	295.89
19	2-Acetylthiazole	3.00	rice, roast	nd	nd	nd	nd	nd	22.38	39.46	30.12
20	(E)-2-Undecenal	0.78	orange, green	824.00	779.96	8.44	1081.94	478.33	19.27	37.01	33.08
21	(E,E)-2,4-Decadienal	0.20	fried, fat	4846.07	2056.00	<1	280.27	132.72	148.83	279.08	242.45

nd, not detected.
1 Important odor-active compounds detected in heated PC, TG, DF, DF-PC, DF-TG, RB, RB-PC, and RB-TG.
2 Odor detection threshold in water. Odor thresholds in water were obtained from Gemert.

ketones, and alcohols being the primary species formed during thermal oxidation. The total content of aldehydes and ketones generated from DF-PC were significantly higher compared to DF-TG.

The trend of aroma compounds produced by thermo-oxidative degradation of DF-PC and DF-TG were essentially similar to the lipids samples. Nonanal and (E)-2-Undecenal were the major aldehydes produced during thermal oxidation of defatted beef with added lipids. The DF-TG produced notably more nonanal than the DF-PC, but less (E)-2-undecenal. However, the DF-PC produced lower concentration of (E,E)-2,4-decadienal and decanal from the thermal reaction than PC samples. The major ketones formed by DF-PC and DF-TG remained 2-nonanone and 2-decanone. In addition, thermal oxidation of DF-PC and DF-TG produced heterocycles such as furans, pyrazines, and pyridines as well as sulfides through the Maillard reaction. The total concentration of sulfides generated from DF-PC were significantly higher than DF-TG. Specifically, the DF-PC thermally reacted to produce higher concentration of 2-pentylpyridine, dimethyl disulfide, and dimethyl trisulfide than the DF-TG.

Seventeen odor-actives compounds (OAV>1) were identified in DF-PC, one more than in DF-TG. The odor-active compounds generated by thermo-oxidative degradation of DF-PC and DF-TG were mainly aliphatic aldehydes, ketones, furans and sulfides. The odor-active compounds produced during thermo-oxidative degradation of the DF-PC and DF-TG were 11 aliphatic aldehydes, 3 ketones, 2 sulfides, and 1 furan. 1-Octen-3-one, nonanal, and (E)-2-undecenal were the odor-active compounds with OAV >1000 generated by the thermal reaction of the DF-PC. In contrast, the odor-active compounds with OAV >1000 generated by the thermal reaction of the DF-TG were only 1-octen-3-one and nonanal.

3.4. Effect of the addition of PC and TG on the aroma-active compounds in raw beef

Principal component analysis revealed that the cumulative contribution rate of the first two principal components reaches 80% (Fig. 4(a)). The concentration of aroma compounds generated from heated raw beef was significantly elevated by the addition of PC and TG. As shown in Fig. 4(b), the total concentrations of aldehydes, ketones, and sulfides generated by heated RB-PC were higher than RB-TG. A total of 64 aroma compounds were detected in heated raw beef with the addition of PC and TG (Fig. 4(c)). Hexanal, heptanal, pentanal, octanal and nonanal were the major aldehydes and 1-octen-3-one was the major ketone produced by heated raw beef, and RB-PC produced higher concentration of pentanal and 1-octen-3-one than RB-TG. In addition, 13 heterocycles and 4 sulfides were generated from heated raw beef. 2-Acetylthiazole was the major heterocycle, while dimethyl disulfide and dimethyl trisulfide were the major sulfides. The concentration of 2-pentylpyridine, 2-acetylthiazole, and dimethyl trisulfide generated from heated RB-PC were higher than RB-PC.

A total of 21 odor-active compounds were identified by GC-O technique in heated raw beef samples (Table 2). It contains 13 aldehydes, 3 ketones, 3 sulfides, and 2 heterocycles. Aldehydes, ketones and sulfides were the major odor-active compounds of heated raw beef, with aldehydes contributing the most to beef aroma (Fig. 4(e)). The odor-actives compounds that contributed to the aroma in the heated RB-PC were hexanal, heptanal, octanal, nonanal, dimethyl disulfide, dimethyl trisulfide, 1-octen-3-one, methional, (E)-2-nonenal, (E)-2-decenal, and (E,E)-2,4-decadienal (OAV>100). Based on the type of aroma, these compounds can be broadly classified into four categories: green, butter, fat, and others (Fig. 4(d)). In addition, methional was identified in heated raw beef samples and was not detected in lipids and defatted beef samples.

4. Discussion

TG and PC not only contribute to aroma formation but also play a role in aroma retention. PC was the major component of beef phospholipids, possesses a choline group and contains a high level of unsaturated fatty acids. PC (P-16:0/18:1), PC (16:0/18:1), and PC (P-16:0/18:2) were the major PC molecules in the fraction2 isolated in this study. PC (16:0/18:1) was the predominant PC molecule in beef, which was similar to the results of this study (Yamamoto et al., 2021). PC molecules are mainly composed of unsaturated fatty acids, such as oleic acid (C18:1) and linoleic acid (C18:2). Linoleic acid positively correlated with the formation of sweet aroma compound γ-hexalactone in beef (Ueda et al., 2021). TG (16:0/18:1/18:1) and TG (16:1/18:1/18:1) were

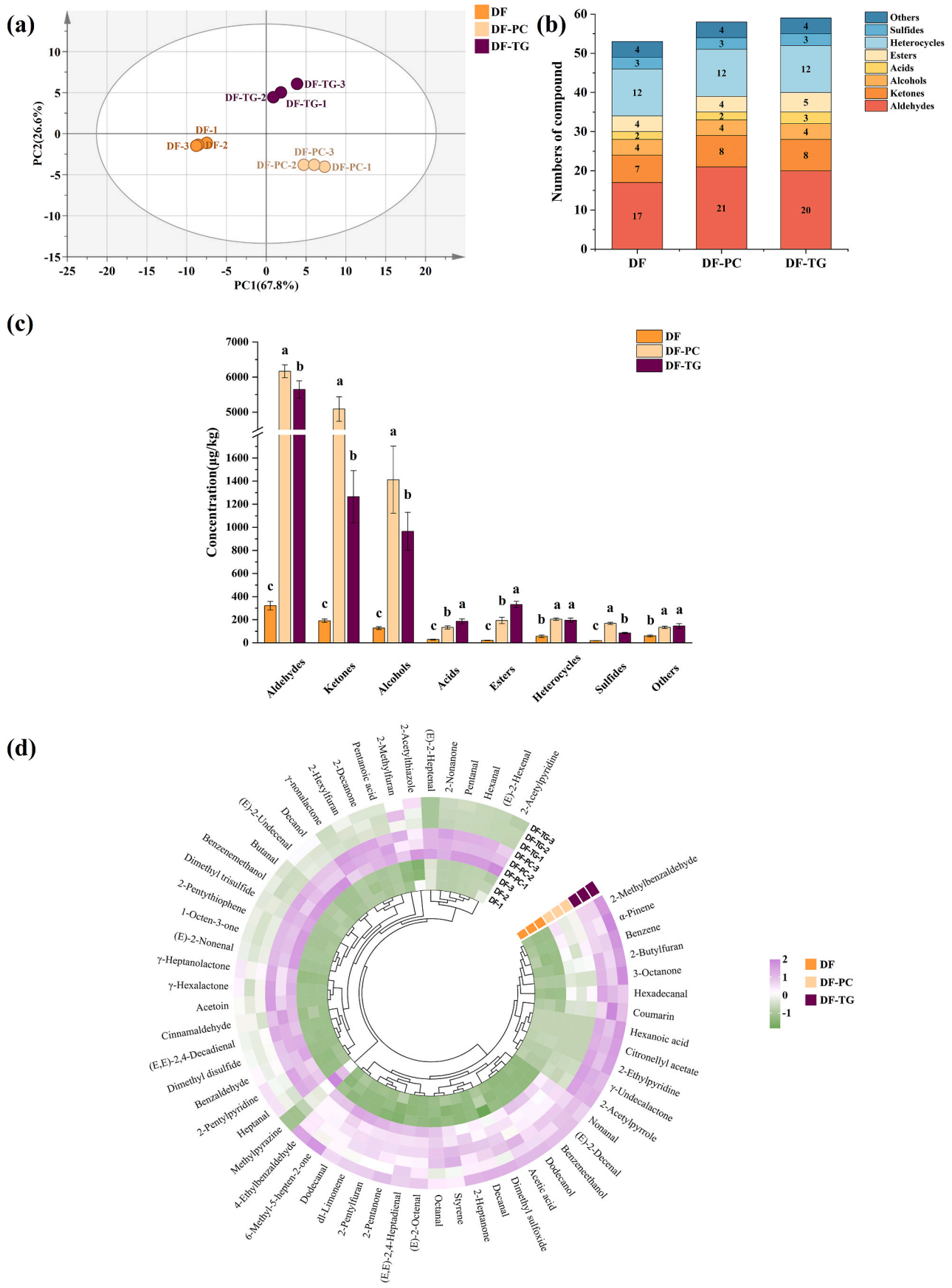

Fig. 3. Analysis of aroma compounds generated by thermal oxidation of DF-PC and DF-TG samples. (a) Two-dimensional PCA score plot. (b) The numbers of aroma compounds. (c) Total concentration of aroma compounds. (d) The circular heatmap of aroma compounds content.

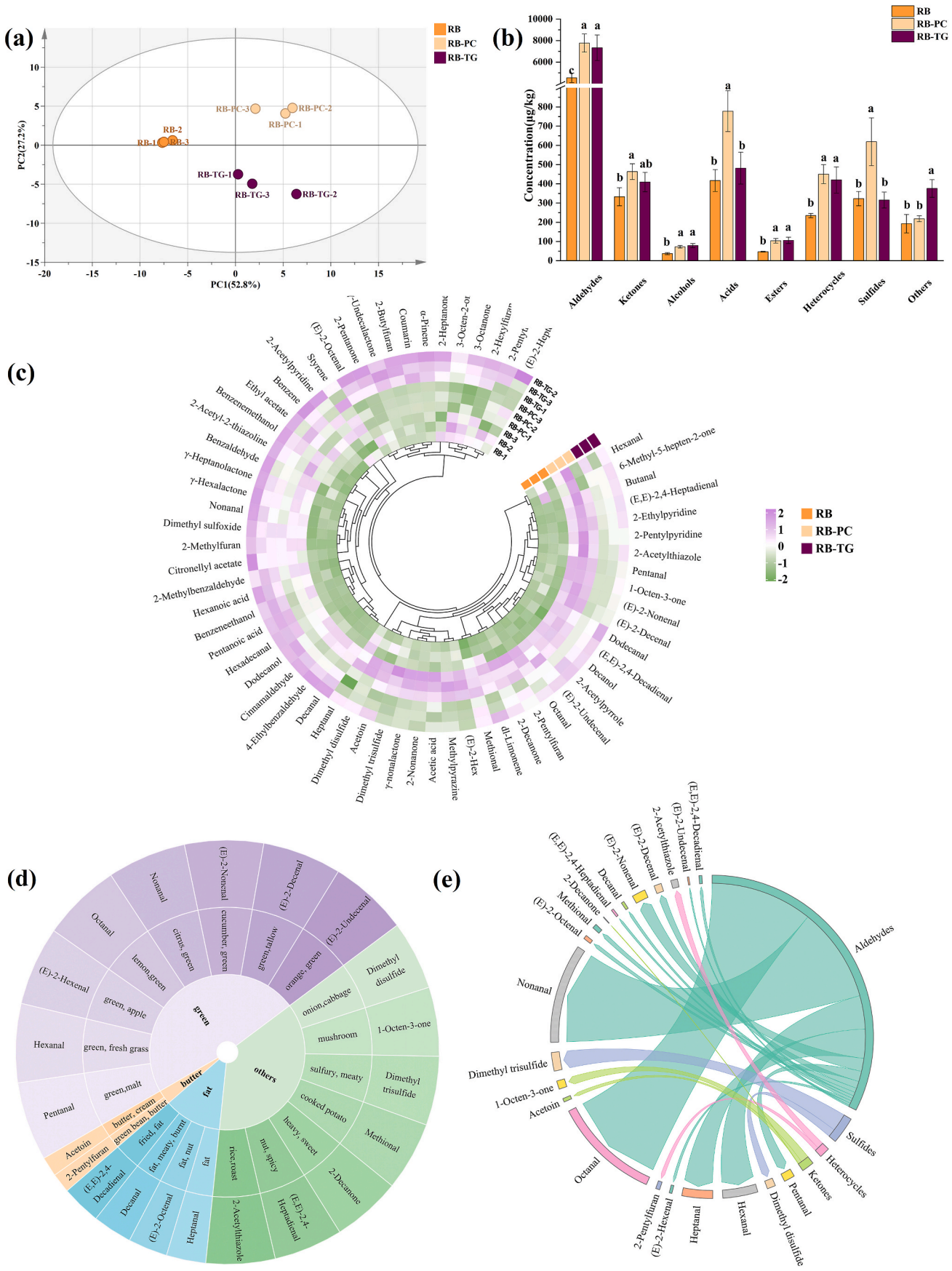

Fig. 4. Analysis of aroma compounds generated by thermal oxidation of RB-PC and RB-TG samples. (a) Two-dimensional PCA score plot. (b) Total concentration of aroma compounds. (c) The circular heatmap of aroma compounds content. (d) Classification of odor-active compounds. (e) Chord plot of odor-active compounds contents.

the major TG molecules isolated from fraction1. TG (16:0/18:1/18:1) was the major lipid molecules responsible for the maintenance of aroma (Li et al., 2024). Additionally, ketones, alcohols, and esters were found to be the predominant volatile compounds in TG. The fatty acids in TG are mainly stearic acid, oleic acid, linoleic acid, and palmitic acid. These saturated fatty acids are more conducive to the formation of alcohols and esters (Li et al., 2021). The fatty acid composition of TG and PC influences their respective contributions to aroma formation. In this study, we isolated and purified PC and TG, and established an in vitro thermal oxidation model using a single lipid. However, there were some limitations in the isolation and identification of the lipids, such as the presence of trace amounts of other phospholipids in the isolated PC (fraction2). Therefore, the methods for isolation and identification could be further optimized.

Aldehydes and ketones are the primary aroma compounds formed during the thermal oxidation of PC and TG. Nonanal, decanal, (E,E)-2,4-decadienal, and 1-octen-3-one were the primary aliphatic compounds contributing to the aroma of beef. PC was rich in unsaturated fatty acids such as C18:1 and C18:2, and it possessed a distinctive choline head group, making it a superior carrier of unsaturated fatty acid compared to TG (Le Grandois et al., 2010; Zhou et al., 2015). Furthermore, the glyceride structure in TG retarded the chain initiation reaction, while its hydroperoxides were spatially blocked. This caused the thermal oxidation process of TG to proceed in stages, which may affect the oxidative decomposition of fatty acid chains within the same TG (Zhou et al., 2022). The decomposition of O-8-hydroperoxide formed by oxidation of C18:1 leads to decanal (Lin et al., 2023). Nonanal can be generated from the β-scission of O-10-hydroperoxide, or through keto-enol tautomerism of the product formed by the combination of 1-nonenyl radical from the decomposition of O-9-hydroperoxide and hydroxyl radical. Heptanal was not a direct product of C18:1 and C18:2 oxidation but may arise from the conversion of heptanol formed by the decomposition of O-11-hydroperoxide (Zhang et al., 2015). (E)-2-Nonenal and (E,E)-2,4-decadienal were formed through the β-scission of alkoxyl radicals derived from 9-hydroperoxy-linoleic acid (Tsuzuki, 2019). However, it was noticeable that the concentration of nonanal generated from thermal oxidation of TG was significantly higher than PC. This result was consistent with the results by Zhou et al., who demonstrated that the choline group in the PC form retards the oxidation of fatty acyl groups compared to TG (Zhou et al., 2014). Ketones have a distinctive aroma, which exerts a significant influence on the aroma of beef. 2-Nonanone and 2-decanone were the primary ketone compounds generated through the thermal oxidation of PC. Specifically, 2-nonanone can impart scents resembling heated milk, soap, green notes, fruity aromas, and floral fragrances, while 2-decanone can contribute fruity notes (Hoa Van et al., 2012). Therefore, the contribution of PC thermo-oxidative degradation to aroma compounds was stronger than TG.

Odor-active compounds with high OAV can significantly impact overall beef aroma. Aldehydes were the primary odor-active compounds generated from lipids oxidation, such as hexanal, decanal, heptanal, octanal, nonanal, (E)-2-undecenal, and (E,E)-2,4-decadienal (Al-Dalali et al., 2022). Nonanal, decanal, (E)-2-nonenal, (E)-2-decenal, and (E)-2-undecenal were highly representative high-level straight-chain aliphatic aldehydes, which were important odor-active compounds involved in the formation of beef aroma. Hexanal, heptanal and octanal were important components in the development of beef fat aroma, all of which contributed to the overall aroma profile of beef (Fang et al., 2024). In this study, decanal, (E)-2-nonenal, (E)-2-undecenal, (E,E)-2,4-decadienal, and 1-octen-3-one were identified as the odor active compounds contributing predominantly to the aroma in the PC samples. While nonanal, (E)-2-undecenal, (E,E)-2,4-decadienal, and 1-octen-3-one were identified in the TG samples as the odor active compounds that mainly contributed to the aroma. Nonanal and (E)-2-undecenal imparted a citrusy aroma, decanal contributed to fatty and meaty notes, and (E)-2-nonenal exhibited green and cucumber-like aromas along with mild fatty notes. (E)-2-decenal generated green and tallowy aroma, and (E,E)-2,4-decadienal produced a distinct fried odor (Wang et al., 2023). 1-Octen-3-one was the primary ketone compound generated from heated PC, imparting a mushroom-like aroma (Tian et al., 2015). Sulfides were important aroma compounds in cooked beef, primarily derived from Maillard reaction products or amino acid pyrolysis. Dimethyl trisulfide exhibited meaty and sulfur notes and methional exhibited roasted potato notes, both of them serving as key odor-active compounds contributing to beef aroma (Zheng et al., 2023). Therefore, aliphatic aldehydes, ketones, and sulfides were the major odor-active compounds produced by the thermal oxidation of PC and TG.

The oxidation of lipids in meat and meat products was a complex process influenced by the complexity of muscle tissue composition. The perception of aroma depended not only on the composition of the aroma compounds but also on the extent to which these compounds were released and retained in the meat matrices (Zhang et al., 2021). Proteins were important components involved in the formation of beef aroma. The distribution of aroma compounds between the lipid and protein fractions in meat matrices is a complex issue. For example, methional had a roasted potato aroma and was detected only in heated raw beef samples. It was due to the fact that α-dicarbonyl compounds produced by the Amadori rearrangement during beef heating could react with amino acids to produce aromatic aldehydes (Wang et al., 2024). The amphipathic nature of phospholipids may account for differences in the concentration of certain aroma compounds in lipid samples, defatted beef samples, and raw beef samples, allowing them to spontaneously form various self-assembled structures in aqueous environments, potentially affecting the reaction pathways (Lin et al., 2004; Pu et al., 2024). Additionally, according to calculations, the surface area of phospholipids per unit weight is over 100 times greater than that of triglyceride droplets. When phospholipids are uniformly dispersed within defatted beef matrices, their surface area increases, thereby altering the rate of lipid oxidation (Wu et al., 2021). This may account for the difference in the trend of PC in defatted beef matrices thermal oxidation alone. Therefore, matrix effects played a crucial role in the lipid thermal oxidation process.

It was reported that the addition of phospholipids could increase the formation of aroma compounds in livestock and poultry products. Addition of phospholipids resulted in a significant increase in (E,E)-2,4-decadienal content in heated chicken meat (Chen et al., 2019). Zheng et al. found that heat-dried Antarctic krill added with PC (16:0/18:2) produced a richer variety and concentration of aroma compounds than those added with PE (18:1/18:1) or PE (18:0/18:0), and the main odor-active compounds produced by the thermal oxidation of PC (16:0/18:2) were hexanal, (E)-2-nonenal, (E)-2-decenal, (E,E)-2,4-nonadienal and (E,E)-2,4-decadienal (Zheng et al., 2022). In addition, a number of studies have shown that PC promotes the formation of Maillard reaction products. After adding phospholipids to the beef bone Maillard reaction model, Zheng observed a significant increase in Maillard reaction products, with sulfide content showing the most pronounced increase, consistent with the findings of this study (Zhang et al., 2021). Zhang et al. found that adding phospholipids significantly increased the concentration of sulfides generated from phospholipid (lecithin and cephalin)-xylose-cysteine reaction systems after heating (Zhang et al., 2021). Thus, the addition of phospholipids could promoted lipid oxidation and the formation of lipid-Maillard reaction products.

5. Conclusion

In this study, PC and TG were isolated and purified from beef and three thermal oxidation models were developed: a single lipid in vitro model, a defatted beef reconstruction model, and a raw beef model. The aroma composition of three thermal oxidation models was then analyzed using the GC-O-MS technique. Decanal, (E)-2-nonenal, (E)-2-undecenal, and (E,E)-2,4-decadienal were the major aroma compounds

produced by the thermal oxidation of PC, while the major aroma compounds produced by the thermal oxidation of TG were nonanal, (E)-2-undecenal and decanal. The aroma composition of defatted beef reconstruction model suggested that the beef matrix inhibited the production of decanal and (E,E)-2,4-decadienal. Furthermore, the addition of PC significantly increased the levels of Maillard reaction products, particularly sulfides, in cooked beef. This study may serve as a reference for developing reconstructed matrices to investigate the effects of thermo-oxidative degradation of lipid molecules on the aroma composition of beef.

CRediT authorship contribution statement

Yujie Shi: Writing – original draft, Visualization, Investigation, Formal analysis. **Jing Li:** Writing – review & editing, Formal analysis. **Longzhu Zhou:** Investigation. **Junmin Zhang:** Supervision, Funding acquisition. **Xiaohui Feng:** Validation, Methodology. **Weihai Xing:** Validation, Methodology. **Chaohua Tang:** Writing – review & editing, Funding acquisition, Conceptualization. **Yueyu Bai:** Supervision, Funding acquisition.

Declaration of competing interest

The authors declare that they have no known competing financial interests or personal relationships that could have appeared to influence the work reported in this paper.

Acknowledgements

This work has been financially supported by National Key R&D Program of China (No. 2023YFD1600102), The Chinese Academy of Agricultural Science and Technology Innovation Project (CAAS-SCAB-202302 and ASTIP-IAS-12), Basal Research Fund for state key laboratory of Animal Nutrition and Feeding (No. 2004DA125184G2407), Natural Science Foundation of Henan (No. 242300421544),The Key Research and Development Program of Henan (No. 241111110100), and The Special Fund for Henan Agriculture Research System (HARS-22-13-Z1).

Appendix A. Supplementary data

Supplementary data to this article can be found online at https://doi.org/10.1016/j.crfs.2025.100973.

Data availability

Data will be made available on request.

References

Al-Dalali, S., Li, C., Xu, B., 2022. Insight into the effect of frozen storage on the changes in volatile aldehydes and alcohols of marinated roasted beef meat: potential mechanisms of their formation. Food Chem. 385, 132629. https://doi.org/10.1016/j.foodchem.2022.132629.

Chen, D., Balagiannis, D.P., Parker, J.K., 2019. Use of egg yolk phospholipids to generate chicken meat odorants. Food Chem. 286, 71–77. https://doi.org/10.1016/j.foodchem.2019.01.184.

Chen, D., Wan, P., Yao, J., Yang, X., Liu, J., 2023. Egg yolk phospholipids as an ideal precursor of fatty note odorants for chicken meat and fried foods: a review. Food Chem. 407, 135177. https://doi.org/10.1016/j.foodchem.2022.135177.

Cui, H., Wang, Y., Liu, X., Wang, Y., Zhang, L., Chen, Y., Jia, Y., Zhao, G., Wen, J., 2023. Identification of common aroma contributors and the regulated metabolites of different kinds of meat. LWT–Food Sci. Technol. 181, 114737. https://doi.org/10.1016/j.lwt.2023.114737.

Elmore, J.S., Mottram, D.S., 2006. The role of lipid in the flavour of cooked beef. Dev. Food Sci. 43, 375–378. https://doi.org/10.1016/S0167-4501(06)80089-0.

Fang, Y., Zhang, J., Ma, C., Xing, L., Wang, W., Zhang, W., 2024. Ultrasound-induced modifications of beef flavor characteristics during postmortem aging. Ultrason. Sonochem. 108, 106979. https://doi.org/10.1016/j.ultsonch.2024.106979.

Gemert, L.J.V., 2011. Compilations of Odour Threshold Values in Air, Water and Other Media, Second Enlarged. Revised Edition): Oliemans Punter & Partners BV.

Hoa Van, B., Inho, H., Dawoon, J., Amna, T., 2012. Principle of meat aroma flavors and future prospect. In: Isin, A. (Ed.), Latest Research into Quality Control. Ch. 7). Rijeka.

Le Grandois, J., Marchioni, E., Ennahar, S., Giuffrida, F., Bindler, F., 2010. Identification and kinetics of oxidized compounds from phosphatidylcholine molecular species. Food Chem. 119 (3), 1233–1238. https://doi.org/10.1016/j.foodchem.2009.08.042.

Li, J., Zhang, Y., Zhang, R., Yang, R., Ma, Q., Wang, Z., Li, P., Xing, J., Gao, P., Liu, H., Gong, H., 2024. Unraveling the formation mechanism of aroma compounds in pork during air frying using UHPLC-HRMS and Orbitrap Exploris GC–MS. Food Res. Int. 192, 114816. https://doi.org/10.1016/j.foodres.2024.114816.

Li, P., Zhao, W., Liu, Y., Zhang, A., Liu, S., Song, R., Zhang, M., Liu, J., 2021. Precursors of volatile organics in foxtail millet (Setaria italica) porridge: the relationship between volatile compounds and five fatty acids upon cooking. J. Cereal. Sci. 100, 103253. https://doi.org/10.1016/j.jcs.2021.103253.

Lin, J., Leser, M.E., Löliger, J., Blank, I., 2004. A new insight into the formation of odor active carbonyls by thermally-induced degradation of phospholipids in self-assembly structures. J. Agric. Food Chem. 52 (3), 581–586. https://doi.org/10.1021/jf035070e.

Lin, X., Wang, S., Wang, Y., Wang, B., Ji, C., Lin, X., Liang, H., Zhang, S., Xu, X., Liang, D., 2023. Density functional theory studies on the oleic acid thermal oxidation into volatile compounds. Food Chem. X 19, 100737. https://doi.org/10.1016/j.fochx.2023.100737.

Lu, Q., Qiu, C., Zhu, J., Liu, J., Wang, X., Guo, X., 2024. Elucidation of key fatty aroma compound contributing to the hepatopancreas of Eriocheir sinensis using sensomics approach by GC-IMS and GC–MS-O. Food Chem. 455, 139904. https://doi.org/10.1016/j.foodchem.2024.139904.

Matyash, V., Liebisch, G., Kurzchalia, T.V., Shevchenko, A., Schwudke, D., 2008. Lipid extraction by methyl-tert-butyl ether for high-throughput lipidomics. J. Lipid Res. 49 (5), 1137–1146. https://doi.org/10.1194/jlr.D700041-JLR200.

Miller, R.K., Luckemeyer, T.J., Kerth, C.R., Adhikari, K., 2023. Descriptive beef flavor and texture attributes relationships with consumer acceptance of US light beef eaters. Meat Sci. 204, 109252. https://doi.org/10.1016/j.meatsci.2023.109252.

Mottram, D.S., Edwards, R.A., 1983. The role of triglycerides and phospholipids in the aroma of cooked beef. J. Sci. Food Agric. 34, 517–522. https://doi.org/10.1002/jsfa.2740340513.

O'Quinn, T.G., Legako, J.F., Woerner, D.R., Kerth, C.R., Nair, M.N., Brooks, J.C., Lancaster, J.M., Miller, R.K., 2024. A current review of U.S. beef flavor II: managing beef flavor. Meat Sci. 209, 109403. https://doi.org/10.1016/j.meatsci.2023.109403.

Pu, D., Shan, Y., Wang, J., Sun, B., Xu, Y., Zhang, W., Zhang, Y., 2024. Recent trends in aroma release and perception during food oral processing: a review. Crit Rev Food Sci 64 (11), 3441–3457. https://doi.org/10.1080/10408398.2022.2132209.

Qi, J., Du, C., Yao, X., Yang, C., Zhang, Q., Liu, D., 2022. Enrichment of taste and aroma compounds in braised soup during repeated stewing of chicken meat. LWT 168, 113926. https://doi.org/10.1016/j.lwt.2022.113926.

Saito, H., 2007. Identification of novel n-4 series polyunsaturated fatty acids in a deep-sea clam, Calyptogena phaseoliformis. J. Chromatogr. A 1163 (1), 247–259. https://doi.org/10.1016/j.chroma.2007.06.016.

Sohail, A., Al-Dalali, S., Wang, J., Xie, J., Shakoor, A., Asimi, S., Shah, H., Patil, P., 2022. Aroma compounds identified in cooked meat: a review. Food Res. Int. 157, 111385. https://doi.org/10.1016/j.foodres.2022.111385.

Tian, H., Li, F., Qin, L., Yu, H., Ma, X., 2015. Quality evaluation of beef seasonings using gas chromatography-mass spectrometry and electronic nose: correlation with sensory attributes and classification according to grade level. Food Anal. Methods 8 (6), 1522–1534. https://doi.org/10.1007/s12161-014-0031-4.

Tsuzuki, S., 2019. Higher straight-chain aliphatic aldehydes: importance as odor-active volatiles in human foods and issues for future research. J. Agric. Food Chem. 67 (17), 4720–4725. https://doi.org/10.1021/acs.jafc.9b01131.

Ueda, S., Sasaki, R., Nakabayashi, R., Yamanoue, M., Sirai, Y., Iwamoto, E., 2021. Exploring the lipids involved in the formation of characteristic lactones in Japanese black cattle. Metabolites 11 (4), 203. https://doi.org/10.3390/metabo11040203.

Wang, D., Wang, J., Lang, Y., Huang, M., Hu, S., Liu, H., Sun, B., Long, Y., Wu, J., Dong, W., 2024. Interactions between food matrices and odorants: a review. Food Chem. 142086. https://doi.org/10.1016/j.foodchem.2024.142086.

Wang, J., Yang, P., Liu, J., Yang, W., Qiang, Y., Jia, W., Han, D., Zhang, C., Purcaro, G., Fauconnier, M.-L., 2024. Study of the flavor dissipation mechanism of soy-sauce-marinated beef using flavor matrices. Food Chem. 437, 137890. https://doi.org/10.1016/j.foodchem.2023.137890.

Wang, Y., Zhang, H., Li, K., Luo, R., Wang, S., Chen, F., Sun, Y., 2023. Dynamic changes in the water distribution and key aroma compounds of roasted chicken during roasting. Food Res. Int. 172, 113146. https://doi.org/10.1016/j.foodres.2023.113146.

Wu, H., Xiao, S., Yin, J., Zhang, J., Richards, M.P., 2021. Impact of lipid composition and muscle microstructure on myoglobin-mediated lipid oxidation in washed cod and pig muscle. Food Chem. 336, 127729. https://doi.org/10.1016/j.foodchem.2020.127729.

Yamamoto, S., Kato, S., Senoo, N., Miyoshi, N., Morita, A., Miura, S., 2021. Differences in phosphatidylcholine profiles and identification of characteristic phosphatidylcholine molecules in meat animal species and meat cut locations. Biosci., Biotechnol., Biochem. 85 (5), 1205–1214. https://doi.org/10.1093/bbb/zbab010.

Zhang, J., Kang, D., Zhang, W., Lorenzo, J.M., 2021. Recent advantage of interactions of protein-flavor in foods: perspective of theoretical models, protein properties and extrinsic factors. Trends Food Sci. Technol. 111, 405–425. https://doi.org/10.1016/j.tifs.2021.02.060.

Zhang, Q., Qin, W., Lin, D., Shen, Q., Saleh, A.S., 2015. The changes in the volatile aldehydes formed during the deep-fat frying process. J. Food Sci. Technol. 52 (12), 7683–7696. https://doi.org/10.1007/s13197-015-1923-z.

Zhang, T., Zhang, K., Qi, X., Lin, S., Qin, L., Huang, X., 2024. Effects of thermal oxidation interaction via various polar lipid and myofibrillar proteins on the aroma formation in large yellow croaker. Food Biosci. 62, 105252. https://doi.org/10.1016/j.fbio.2024.105252.

Zhang, Z., Zang, M., Zhang, K., Wang, S., Li, D., Li, X., 2021. Effects of phospholipids and reheating treatment on volatile compounds in phospholipid-xylose-cysteine reaction systems. Food Res. Int. 139, 109918. https://doi.org/10.1016/j.foodres.2020.109918.

Zhao, J., Wang, T., Xie, J., Xiao, Q., Cheng, J., Chen, F., Wang, S., Sun, B., 2019. Formation mechanism of aroma compounds in a glutathione-glucose reaction with fat or oxidized fat. Food Chem. 270, 436–444. https://doi.org/10.1016/j.foodchem.2018.07.106.

Zheng, A., Wei, C., Liu, D., Thakur, K., Zhang, J., Wei, Z., 2023. GC-MS and GC×GC-ToF-MS analysis of roasted/broth flavors produced by Maillard reaction system of cysteine-xylose-glutamate. Curr. Res. Food Sci. 6, 100445. https://doi.org/10.1016/j.crfs.2023.100445.

Zheng, X., Ji, H., Liu, S., Shi, W., Lu, Y., 2025. Shrimp lipids improve flavor by regulating characteristic aroma compounds in hot air-dried shrimp. Food Chem. 465, 142065. https://doi.org/10.1016/j.foodchem.2024.142065.

Zheng, X., Ji, H., Zhang, D., Zhang, Z., Liu, S., Song, W., 2022. The identification of three phospholipid species roles on the aroma formation of hot-air-dried shrimp (Litopenaeus vannamei) by gas chromatography–ion mobility spectrometry and gas chromatography- mass spectrometry. Food Res. Int. 162, 112191. https://doi.org/10.1016/j.foodres.2022.112191.

Zhou, L., Ren, Y., Shi, Y., Fan, S., Zhao, L., Dong, M., Li, J., Yang, Y., Yu, Y., Zhao, Q., Zhang, J., Tang, C., 2024. Comprehensive foodomics analysis reveals key lipids affect aroma generation in beef. Food Chem. 461, 140954. https://doi.org/10.1016/j.foodchem.2024.140954.

Zhou, L., Zhao, M., Bindler, F., Marchioni, E., 2014. Comparison of the volatiles formed by oxidation of phosphatidylcholine to triglyceride in model systems. J. Agric. Food Chem. 62 (33), 8295–8301. https://doi.org/10.1021/jf501934w.

Zhou, L., Zhao, M., Bindler, F., Marchioni, E., 2015. Identification of oxidation compounds of 1-Stearoyl-2-linoleoyl-sn-glycero-3-phosphoethanolamine during thermal oxidation. J. Agric. Food Chem. 63 (43), 9615–9620. https://doi.org/10.1021/acs.jafc.5b03753.

Zhou, Z., Li, Y., Zhao, F., Xin, R., Huang, X., Zhang, Y., Zhou, D., Qin, L., 2022. Unraveling the thermal oxidation products and peroxidation mechanisms of different chemical structures of lipids: an example of molecules containing oleic acid. J. Agric. Food Chem. 70 (51), 16410–16423. https://doi.org/10.1021/acs.jafc.2c06221.